### Design, Synthesis, and Biological Evaluation of Benzofuran Derivatives as Inhibitors of Inflammatory Enzymes in Kidney Cancer Therapy

Afyaa M. Younus\*, Adnan O. Omar, Mohammed B. Hassin Department of Chemistry, College of Science, University of Mosul, Mosul, Iraq

#### Abstract

The present study employed Ultra sound technique to prepare three novel organic compounds. These compounds share a structural similarity with curcumin (A). Specifically, the compounds included the unsubstituted form (B), a 6-OMe-substituted derivative (C), and a 5-Br-substituted derivative (D). The study examined the potential efficacy of selected compounds against kidney cancer in mice through molecular docking approaches. Docking studies revealed that these compounds exhibited strong interactions with four key enzymes involved in inflammation: TNF-alpha, COX-2, IL-6, and LOX-2. Notably, these compounds demonstrated the lowest (most negative)  $\Delta G$ values, indicating effective inhibition of these enzymes. The results confirmed that the synthesized compounds displayed substantial binding affinity and inhibitory effects on these enzymes. Following molecular docking analysis, an in vivo study was carried out using 90 male mice, randomly assigned to six groups (5 per group). The control group received a standard diet and distilled water, while groups 2 through 6 were administered intraperitoneal injections of N-Nitrosodimethylamine (NDMA) at a dose of 60 mg/kg for two months to induce renal carcinogenesis. Subsequently, groups 3 to 6 received additional intraperitoneal treatments with compounds A, B, C, and D at doses of (0.5, 1.0, and 1.5) mg/kg for 21 consecutive days. Biochemical assessments indicated that compound C exerted significant anticancer activity, demonstrated by a marked reduction in TNF-α levels and inhibition of COX-2, IL-6, and LOX-2 enzymes. These molecular changes were associated with amelioration of renal cancer-induced damage. Histopathological examination further confirmed the therapeutic efficacy of compound C, revealing complete regression of renal tumors.

**Keywords**: Benzofuran, Curcumin, N-Nitrosodimethylamine, Lipo-oxygenase.

#### Introduction

Curcumin has been widely explored as a precursor for synthesizing novel bioactive due to compounds [1] its diverse pharmacological properties. Despite its wellestablished therapeutic potential, curcumin's applications are hindered clinical challenges such as poor bioavailability, rapid metabolic degradation, and limited cellular uptake. To address these limitations, extensive research efforts have been directed toward the development of curcumin analogs advanced drug delivery systems. These aim to improve its stability, strategies

absorption, and overall efficacy, particularly in the field of cancer therapy, where curcuminderived compounds have shown promising anti-tumor activity [2], and cancer is a serious medical condition resulting from uncontrolled and abnormal growth of cells in the body [3, 4]. Among the various treatment strategies available, chemotherapy remains a widely used approach [6], involving the administration of organic chemical compounds to target and eliminate cancer cells [7].

Cancer is a genetic condition that occurs when normal cellular processes, particularly

 those involved in cell division, are disrupted, leading to several molecular changes that transform normal cells into cancerous ones. It is defined by the uncontrolled growth and dissemination of abnormal cells, which occurs when the regulatory mechanisms governing division fail. This uncontrolled cell proliferation forms a mass of abnormal cells called a tumor, which may be either benign or malignant [8]. The numbers of cancer patients and cancer deaths are increasing worldwide, and these numbers were estimated to be 18.1 and 9.6 million, respectively, in 2018. Various anticancer agents, such as molecular-targeted drugsand immune checkpoint inhibitors, are currently beingactively developed worldwide. However, considerableamounts of time and money are required to develop an anticancer drug. Therefore, drug repositioning, which aims to find new uses for existing drugs, has attracted the attention of pharmaceutical researchers due to its high efficiency [9]. Kidney cancer, primarily renal cell carcinoma (RCC), accounts for approximately 90% of all kidney malignancies. It is the seventh most common cancer in men and the tenth in women worldwide. originates from the proximal tubular epithelium of the kidney and characterized by genetic mutations, dysregulation, and metabolic a highly immunosuppressive tumor microenvironment. The incidence of kidney cancer has been rising, partly due to improved imaging techniques and risk factors such as obesity, hypertension, and smoking [10].

In this study, we synthesized novel benzofuran-based organic compounds, known for their diverse biological activities, including anti-inflammatory [11] anti-alzheimer's [12], and anticancer effects [13]. A computational investigation was performed using the MCULE molecular docking software to predict their interactions with specific proteins. This analysis included calculating Gibbs free energy ( $\Delta G$ ) and visualizing the binding interactions in both 2D and 3D

formats. The strength and nature of these molecular interactions varied among the synthesized compounds [14]. To further assess their biological impact, we employed an in vivo model by inducing kidney cancer in mice Nthe administration of through via Dimethylnitrosamine (NDMA) the peritoneal cavity [15]. The synthesized compounds were converted into suitable chemical formulations and administered to the mice, followed by biochemical assessments and histopathological examinations. findings revealed that these benzofuran derivatives exhibited a significant influence on kidney cancer progression. The primary goal of this study is to explore and evaluate the therapeutic potential of these newly developed compounds. The synthesized compounds were evaluated by analyzing the serum levels of TNF-α, COX-2, IL-6 and LOX-2 in white mouse with (NDMA)-induced kidney cancer. Molecular docking simulations using the MCULE program demonstrated interactions between these compounds and the target Furthermore, histopathological enzymes. assessments were conducted to investigate tissue modifications, while enzyme levels were monitored throughout the study to evaluate the biochemical effects of the treatment.

#### **Molecular Docking Analysis**

The binding affinities and interaction profiles of the antitumor derivatives (A, B, C, and D) with cancer- related targets TNF-α, COX-2, IL-6, and LOX-2 were explored through molecular docking studies conducted using the MCULE platform and visualized with BIOVIA Discovery Studio (2021). The 3D structures of these proteins were obtained from the Protein Data Bank (PDB) and subjected to molecular docking analysis [16]. MCULE docking was employed to assess the activity of biological the synthesized compounds by calculating the binding free energy ( $\Delta G$ ), which reflects interaction stability and potential enzymatic effects [17]. Additionally, 2D and 3D interaction models were generated to visualize enzyme-ligand binding. To validate these findings, an in vivo study was conducted in which kidney cancer was induced in white mice using NDMA [18]. The levels of TNF-α, COX-2,IL-6 and LOX2 in serum were monitored, while histopathological analysis was performed to

evaluate tissue alterations, providing valuable insights into the therapeutic potential of these compounds.

#### **Materials and Methods**

Starting with Curcumin A (Figure 1, structure below) to prepare the compounds B, C, and D.

Figure 1. Chemical Structure of Curcumin (A)

# Preparation of Starting Material (B, C, D)

# Preparation of [1,7-bis(benzofuran-2-yl) hepta-1,6-diene-3,5-dione]and derived [19]

The first step is to prepare of the 4-(benzofuran -2yl) but-3-en-2-one initial chalcone through the reaction of acetone (0.01mole)/(15ml) ethanol, then (0.01mole) piperidine is added as a base, stirred continuously for (15min), then (0.01mole) benzofuran 2-carbaldehyde dissolved in (10ml)ethanol are added using ultrasound technology at (70 °C) / ZrOCl<sub>2</sub>.8H<sub>2</sub>O as a

catalyst. Then filtrate and recrystallized from EtOH. second step is to prepare of the Ethyl 3-(benzofuran -2yl)acrylate involving reaction of ethyl acetate (0.01mole) dissolved in(15ml) ethanol, using the piperidine base(0.01mole) and stirring for (15min), then (0.01mole) benzofuran 2-carboaldehyde dissolved in (10ml)ethanol are added using ultrasound technology at (70 °C) using ZrOCl<sub>2</sub>.8H<sub>2</sub>O as a catalyst, The product washed by water for times recrystallized from EtOH, then mixture product step 1 and product step2 by condensation reaction (Figure 2).

**Figure 2.** Preparation of [1,7-bis(benzofuran-2-yl) hepta-1, 6-diene-3,5-dione]

#### **Chemical Material Used**

In this study, commercially available ELISA kits were employed to quantify serum

levels of TNF-α, COX-2, IL-6, and LOX-2, following the protocols provided by the respective manufacturers (Table 1).

Table 1. Summarizes the Binding Energies of Anti-inflammatory Derivatives (A-D) with Four Target Proteins

Ligand	TNF- α	COX-2	IL-6	LOX-2	
	[Kcal/mol]	[Kcal/mol]	[Kcal/mol]	[Kcal/mol]	
A	-10.0	-9.6	-6.9	-9.2	
В	-11.4	-11.2	-8.9	-9.2	
С	-10.6	-10.3	-8.6	-9.8	
D	-10.7	-10.6	-8.5	-9.3	

#### **Animals Used**

The study involved 90 white mice, aged 6 weeks, with an average weight 25 grams, The mice were randomly assigned into six equal groups. Each group was housed in separate plastic cages (10 × 20 × 40 cm), each containing five animals. animals were housed in appropriately equipped cages with unrestricted access to food and water. A one-week acclimatization period was observed under standardized laboratory conditions of light and temperature before commencing injections and compound administration.

### **Determining of Inducing Kidney Cancer Dose**

The dosage selected for kidney cancer induction was determined based on protocols established in inter nationally recognized scientific studies. Accordingly, a dose of NDMA(is a known animal carcinogen, and has been shown to induce multiple tumor types, including renal tumors [20,21]. Experimental models for the sequential analysis of chemically-induced renal carcinogenesis. Toxicologic pathology, 14(1), 112-122. at a concentration of 60mg/kg through the peritoneal cavity was administered over a period of two months. Dosage calculations and the preparation of stock solutions for the novel organic compounds were conducted in accordance with established experimental protocols [22]. Stock solutions were prepared to deliver selected doses of 0.5, 1.0, and 1.5

mg/kg. For example, to administer a dose of 1.5 mg/kg to a mouse weighing 25 g, the calculation was as follows: the animal's body weight (25 g) corresponds to 0.0375 mg of the compound, which was dissolved in 0.1mL of DMSO. The required volume of stock solution was scaled accordingly to accommodate the number of animals used in the experiment.

Dosage in (mg)=(Body weight of animal (g))/1000(g) ×dose(mg)

Dosage in  $(mg)=(25 (g))/1000(g) \times 1.5(mg)=0.0375$ 

Animals can be calculated by multiplying both sides by constant value as follows.

0.0375 mg = 0.1 mL

5 mice in each group

the number of days to give a dose=21.

 $21 \times 5 \times 0.0375 \text{ mg} = 21 \times 5 \times 0.1 \text{ mL}$ 

3.93mg of novel organic compounds will be dissolved in 10.5 mL of DMSO = X

Experimental design

X=(3.937(mg))/(10.5 ml)=0.374 mg/ml

The newly developed compound exhibits a strong binding interaction with LOX-2, resulting in its effective inhibition, as demonstrated by the 2D-3D binding model. This interaction suggests that the compound acts as a potent inhibitor of kidney cancer, as LOX-2 plays a crucial role in the tumorigenesis and metastasis of cancer cells.

By inhibiting LOX-2, the compound potentially disrupts cancer cell progression and invasiveness, making it a promising

therapeutic agent for kidney cancer treatment (figure 3).

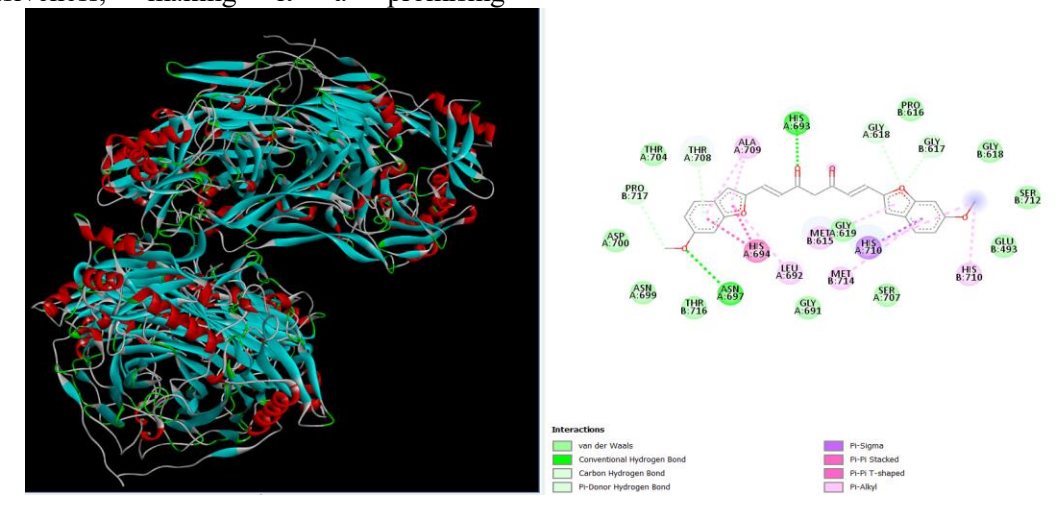


**Figure 3.** 3D and 2D Representations Illustrating the Potential Interactions between Compound C and the LOX-2 Enzyme

The new compound demonstrated high efficacy in inhibiting IL-6, as shown in the corresponding images. IL-6 is a proinflammatory cytokine that plays a critical role in promoting tumor growth and progression. By inhibiting IL-6, the compound can

potentially reduce inflammation within the tumor microenvironment, which is known to support cancer cell survival and proliferation, thus lowering the risk of cancer progression (Figure 4).

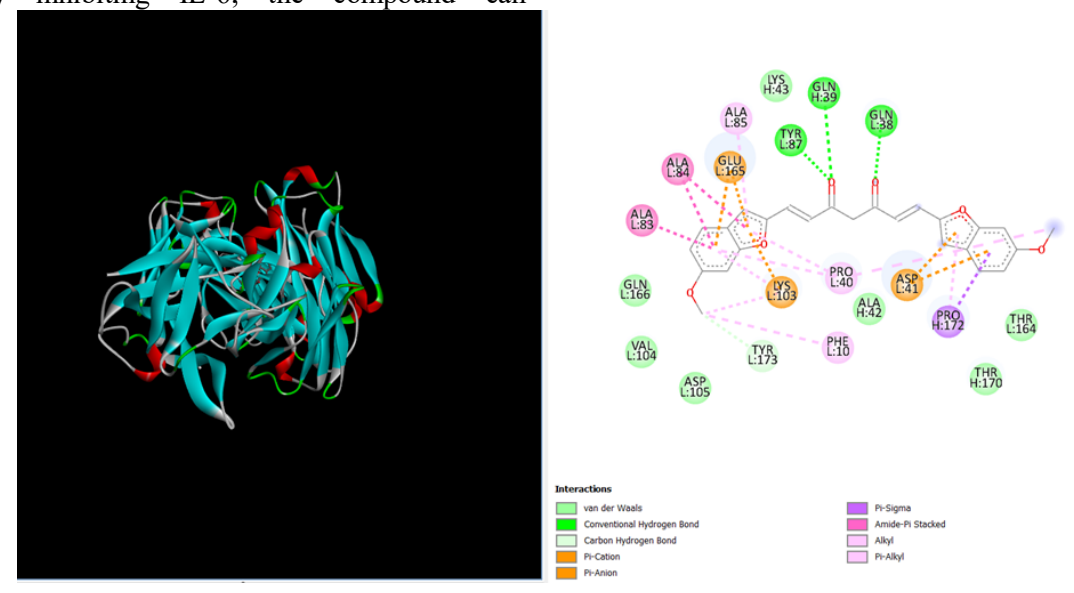


**Figure 4.** 3D and 2D Representations Illustrating the Potential Interactions between Compound C and the IL-6 Protein

Additionally, the compound showed significant inhibition of COX-2, as illustrated by the relevant images. COX-2 is an enzyme that is overexpressed in many types of cancer, contributing to inflammation, angiogenesis,

and tumor cell proliferation. By inhibiting COX-2, the compound helps to reduce these pro-cancerous processes, thereby offering a potential therapeutic effect against cancer (Figure 5).

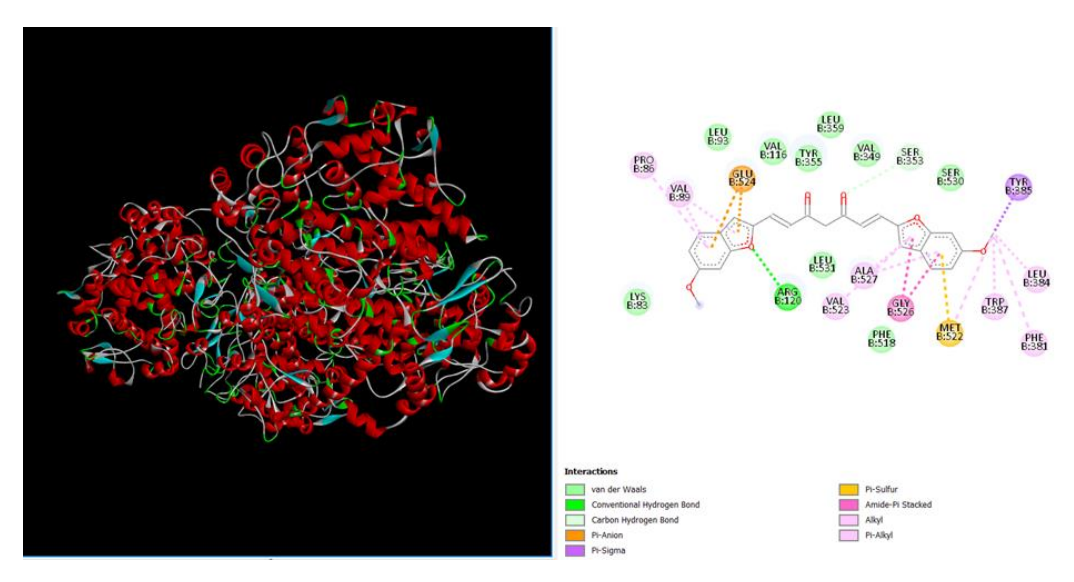


**Figure 5.** 3D and 2D Representations Illustrating the Potential Interactions between Compound C and the COX-2 Enzyme

Furthermore, the compound effectively inhibited TNF- $\alpha$ , as depicted in the images. TNF- $\alpha$  is a cytokine involved in inflammatory responses and is associated with the development of cancer. High levels of TNF- $\alpha$  contribute to tumorigenesis and metastasis. By

targeting and inhibiting TNF- $\alpha$ , the compound could disrupt the inflammatory pathways that facilitate cancer progression, making it a promising candidate for cancer treatment (Figure 6).

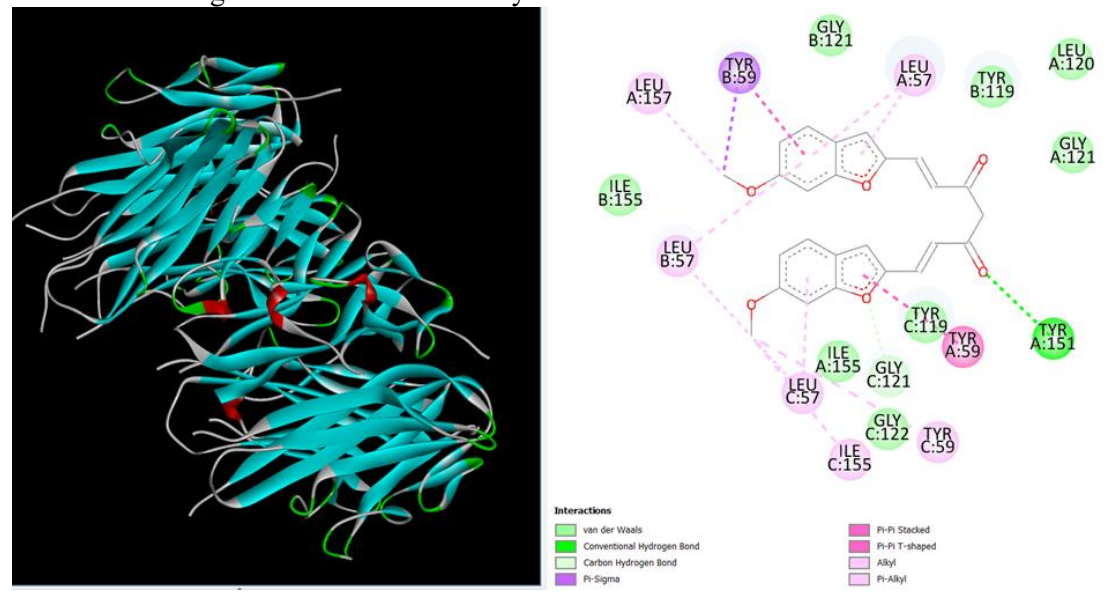


**Figure 6.** 3D and 2D Representations Illustrating the Potential Interactions between Compound C and the TNF- $\alpha$  protein

The animals were randomly assigned into six groups, each comprising five healthy mice, and were maintained on a standard diet throughout the experimental period. One of the groups was subjected to daily intraperitoneal administration of N-Nitrosodimethylamine (NDMA) for two months to induce renal

carcinogenesis. The grouping and treatment protocol were as follows:

**Group I:** (Control): Received only a standard diet and distilled water for the entire duration of the experiment, without any chemical exposure.

**Group II:** Administered NDMA intraperitoneally at a dose of 60 mg/kg for two consecutive months, followed by an additional treatment with DMSO during the final week.

Group III: Treated with NDMA as in Group II, followed by intraperitoneal injections of a novel synthetic compound (A) for 21 days at therapeutic doses of 0.5, 1.0, and 1.5 mg/kg/day.

**Group IV:** Received NDMA for two months, then treated with compound (B) intraperitoneally for 21 days at doses of 0.5, 1.0, and 1.5 mg/kg/day.

**Group V:** Administered NDMA for two months, followed by compound (C) delivered intraperitoneally for 21 days at the same therapeutic doses (0.5, 1.0, and 1.5 mg/kg/day).

**Group VI:** Treated with NDMA for two months, then received compound (D) intraperitoneally for 21 days at doses of 0.5, 1.0, and 1.5 mg/kg/day.

### **Collection of Blood and Kidney Samples**

After completing the experiment, the animals were anesthetized using ether due to its rapid onset and wide safety margin, making it suitable for research applications. Blood samples were collected from the orbital sinus using capillary tubes. The collected blood was transferred into plain tubes without anticoagulants. After allowing the drawn blood to coagulate, the serum was separated using centrifugation for 15 minutes at a speed of (1179 xg). The obtained serum was then carefully aliquoted into specialized tubes and stored at -10 °C until further analysis. Subsequent assays included the measurement of TNF-α, COX-2, LOX-2, and IL-6 levels.

#### **Statistical Analysis**

Statistical analysis was performed by expressing the biochemical parameters as mean  $\pm$  standard deviation, and the Duncan Test was used with ANOVA analysis to

analyze the impact of the studied biochemical variables [23].

#### **Results**

### Assessment of Tumor Necrosis Factoralpha (TNF-α) Levels

The study findings indicate a significant increase (P $\leq$ 0.05) in TNF- $\alpha$  levels in (NDMA)- induced mice compared to the control group, likely due to immune cell activation in response to cancer presence and chronic inflammation associated with kidney cancer [23]. Furthermore, the sustained inflammatory response typically linked to kidney cancer is a key factor contributing to increased TNF- $\alpha$  levels. This inflammation promotes the secretion of TNF-α by immune cells and various other cell types within the tumor microenvironment [24, 22]. However, treatment with doses A, B, C, and D resulted in a significant reduction in TNF-α levels, with compound C exhibiting the highest efficacy. This reduction is attributed to strong binding interactions between the compound and the enzyme, as predicted by molecular docking, which revealed four hydrogen bonds and the most favorable binding energy ( $\Delta G = -10.6$ ), indicating potent enzyme inhibition (Table 2).

## Assessment of Cyclooxygenase-2 (Cox-2) Levels

The findings revealed a significant increase (P < 0.05) in COX-2 concentration in the NDMA-induced group compared to the control. This elevation is likely linked to the activation of intracellular signaling cascades in renal cancer cells, leading to upregulated COX-2 synthesis and secretion. Chronic inflammation in the kidney often resulting from conditions such as recurrent urinary tract infections, nephrolithiasis, or urolithiasis may further contribute to this upregulation. Proinflammatory mediators generated in such pathological contexts are known to enhance COX-2 expression [25]. The study demonstrated a significant reduction in COX-2 concentration in mice treated with different doses, particularly A, B, C, and D, compared to the (NDMA) -induced group. This reduction is attributed to the inhibitory interaction of the compounds with the enzyme [23]. Notably, compound C exhibited the most pronounced effect, due to its strong binding affinity, which was theoretically predicted through molecular docking. The analysis revealed four hydrogen bonds and additional interactions contributing to this stability. Furthermore, the high negative  $\Delta G$  value (-10.3) confirms the compound's potent inhibitory activity [26-28] (Table 2).

# Assessment of Interleucein-6 (IL-6) Levels

A significant elevation in IL-6 concentration (P  $\leq 0.05$ ) was detected in NDMA-induced mice relative to the control group. This rise is likely associated with the activation of specific intracellular signaling involved pathways in renal cancer development [29], which stimulate the production and release of IL-6. Genetic alterations or abnormalities within cancer cells could also contribute to this effect Furthermore, the tumor microenvironment plays a critical role in cancer progression, with immune cells and other stromal components within the kidney tumor either producing IL-6 directly or promoting its secretion [30] (Table 2). Conversely, a significant reduction in IL-6 levels was detected in mice treated with different doses (A, B, C, and D) compared to the (NDMA) -induced group. This decline is likely due to the potent inhibitory effects and strong binding interactions of the tested compounds. Among these, compound C demonstrated the highest efficacy, evidenced by the most substantial reduction in

IL-6 levels. This effect is primarily attributed to the strong binding interactions between the compound and the target enzyme [23], as predicted by molecular docking studies. The binding involves four hydrogen bonds along with additional interactions, contributing to the compound's high affinity. Moreover, compound C exhibited the most negative free energy change ( $\Delta G = -8.6$ ), indicating a strong and efficient inhibitory activity (Table 2).

#### **Assessment of LOX-2 Levels**

The results demonstrated a significant elevation (P  $\leq$  0.05) in LOX-2 levels in the NDMA-induced group compared to the control group. This increase may be attributed to the activation of signaling pathways within renal carcinoma cells, which promote the expression and secretion of LOX-2 [31]. Furthermore, chronic kidney inflammation commonly linked to conditions such as recurrent urinary tract infections, bladder stones, or kidney stones may contribute to the LOX-2. upregulation of Inflammatory mediators released during such pathological states are known to stimulate LOX-2 production [32]. The study demonstrated a significant reduction in LOX-2 concentration treated with different doses, mice particularly A, B, C, and D, compared to the (NDMA) -induced group. This reduction is attributed to the inhibitory interaction of the compounds with the enzyme [23]. Notably, compound C exhibited the most pronounced effect, due to its strong binding affinity, which was theoretically predicted through molecular docking. The analysis revealed four hydrogen bonds and additional interactions contributing to this stability. Furthermore, the high negative  $\Delta G$  value (-9.8) confirms the compound's potent inhibitory activity (Table 2).

**Table 2.** Measured Biochemical Markers Assessed in the Serum Samples of Mice Treatment with (NDMA) and the used Compound A, B, C, and D

	Biochemical markers	Control	Mice induced by NDMA 60mg/kg	Dose (0.5mg/kg)	Dose (1 mg/kg)	Dose (1.5 mg/kg)
A	TNF-α	12.08 ±1.18 e	521.73±1.50a	238.22±5.6c	120.86±2.60 d	261.74±3.91 b
	IL-6	5.13±1.03 d	41.74±0.94a	30.78±1.19 b	24.37±1.39 c	30.49±1.38 b
	COX-2	15.41±1.71 e	404.35±1.83 a	260.81±4.09c	153.23±6.83d	285.34±5.20b
	LOX-2	102.16 ±1.26 e	837.85±3.67 a	323.02±2.72b	292.27±1.31 d	305.92±3.72 c
В	TNF-α	12.08±1.182e	521.73±1.50a	132.15±1.85c	125.86±3.99d	164.34±4.03b
	IL-6	5.134±1.034 e	41.74±0.94a	24.35±1.35c	18.592±1.65d	29.08±1.17b
	COX-2	15.41±1.710e	404.35±1.836a	165.02±6.26c	128.05±5.76d	187.31±2.86b
	LOX-2	102.16±1.26e	837.85±3.67a	213.98±3.56c	205.86±4.52d	227.40±3.26b
C	TNF-α	12.08±1.18d	521.73±1.50a	76.08±10.98c	20.24±3.21d	90.43±8.22b
	IL-6	5.134±1.034d	41.74±0.94a	8.892±0.56b	6.80±0.30c	8.412±0.97b
	COX-2	15.41±1.71e	404.35±1.83a	58.02±1.95b	17.82±1.59d	46.61±1.49c
	LOX-2	102.16±1.26e	837.85±3.67a	194.11±3.27b	109.61±1.57d	125.34±3.35d
D	TNF-α	12.08±1.18 e	521.73±1.50 a	113.87±2.35 b	95.11±3.60 d	101.09±2.18c
	IL-6	5.134±1.03 d	41.74±0.94 a	17.52±1.49b	13.92±1.198c	18.10±1.57b
	COX-2	15.41±1.71 e	404.35±1.836a	105.00±2.89c	91.59±1.63 d	123.97±2.22b
	LOX-2	102.16±1.26e	837.85±3.67 a	314.69±2.97b	280.90±2.02 d	294.54±3.03c

The values are expressed as mean  $\pm$  standard deviation.

Distinct letters denote statistically significant differences at a probability level of  $P \le 0.05$ .

#### **Histological Study**

A histological study of mouse kidney treated with (NDMA) and new synthetic compounds [23].

**Group I**: The results demonstrated a histologically normal kidney architecture. Both the mucosal and submucosal layers were intact, exhibiting well-defined boundaries and no signs of structural damage. The transitional epithelium retained its typical morphology, and the muscular layer appeared unaffected, without any observed damage as seen in diseased conditions (Figure 7).

Group II: In contrast, marked histopathological alterations were observed following NDMA administration, These changes included luminal stenosis, necrosis, and desquamation of the transitional epithelial

cells, along with muscular layer thickening and notable infiltration of inflammatory cells (Figure 7).

Group III: This group received NDMA followed by treatment with compound (A) for 21 days. Histological analysis showed that the tissues were free of any form of damage when compared to the NDMA-only group. Observations included isolated instances of epithelial cell degeneration and necrosis, slight mucosal thinning, and mild inflammatory cell infiltration, indicating a noticeable therapeutic effect of compound (A) (Figure 7).

**Group IV:** Animals in this group were administered NDMA followed by treatment with compound (B) for 21 days. The findings revealed both theoretical and practical evidence of therapeutic efficacy, as the kidney tissue maintained its normal histological

architecture. The mucosal layer lined with transitional epithelium, as well as the submucosal and muscular layers, remained structurally intact and closely resembled those of the control group. Importantly, no histopathological signs of tissue damage were detected, highlighting the protective effects of compound (B) (Figure 7).

Group V: Animals in this group received NDMA followed by treatment with compound (C) for 21 days. Histological examination revealed signs of tissue repair in the kidney, characterized by mild mucosal thinning, limited focal infiltration of inflammatory cells within the submucosa, and limited instances of

cellular degeneration and necrosis epithelial cells. These findings indicate a clear therapeutic effect of compound (C) (Figure 7).

Group VI: Animals in the sixth group were administered NDMA to induce renal damage, followed by treatment with compound (D) for Histopathological analysis days. demonstrated a positive therapeutic response, evidenced by prominent vacuolar degeneration, mild necrosis of the transitional epithelial cells, and vascular congestion. These findings suggest a moderate level of treatment efficacy compared to the untreated NDMAinduced condition (Figure 7).

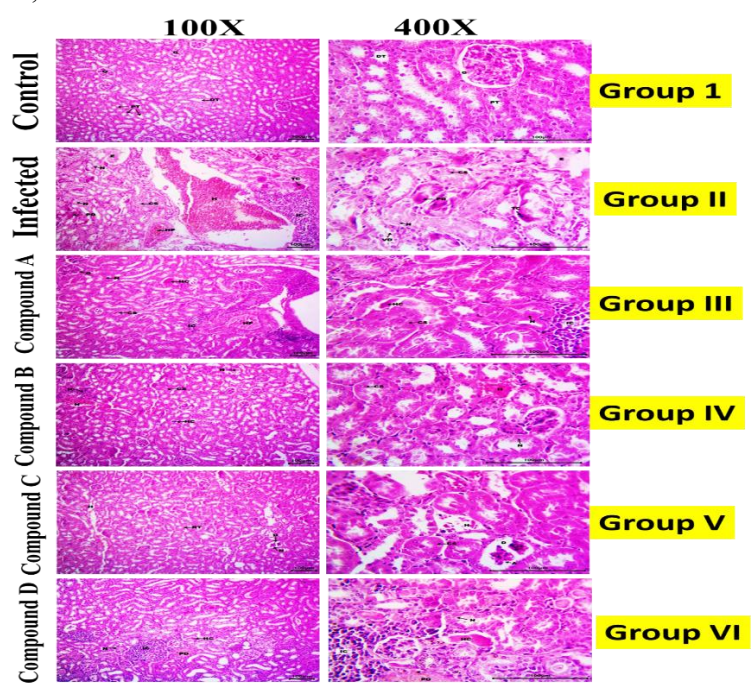


Figure 7. A histological study of mouse kidney treated with (NDMA) and new synthetic compounds (A) Photomicrograph of mice kidney from control (healthy) group demonstrates intact histological architecture of glomeruli, distal renal tubules, and proximal renal tubules. (B) Photomicrograph of mice kidney from control (infected) group demonstrates sever lesions as nephritis representing by polymorph-nuclear and mono-nuclear inflammatory cells, suspected cluster of tumor cells, necrosis, and cell swelling of epithelial cells lining renal tubules, pretentious material deposition, edema, hyperemia, and hemorrhage. (C) Photomicrograph of rat kidney from A compound demonstrates mild inflammatory cells infiltration, mild necrosis, and cell swelling of epithelial cells lining renal tubules, hyaline casts, and hyperemia. (D) Photomicrograph of rat kidney from B compound demonstrates few inflammatory cells infiltration, mild necrosis, and cell swelling of epithelial cells lining renal tubules, hyaline casts, hemorrhage. (E) Photomicrograph of rat kidney from C Compound demonstrates mild atrophy of glomerulus and mild dilation of Bowman's space, hemorrhage with intact renal tubules. (F) Photomicrograph of rat kidney from D compound demonstrates focal inflammatory cells infiltration, mild necrosis of epithelial cells lining renal tubules, hyaline casts, and pretentious material deposition.

#### **Discussion**

study demonstrates The present significant therapeutic potential of novel benzofuran derivatives in targeting inflammatory pathways associated with kidney cancer progression. The NDMA-induced kidney cancer model successfully replicated the chronic inflammatory microenvironment characteristic of renal carcinomas, evidenced by the substantial elevation of key inflammatory biomarkers including TNF-α, COX-2, IL-6, and LOX-2 compared to control groups. This inflammatory cascade represents a critical mechanism in kidney cancer pathogenesis, sustained where immune activation and the release of pro-inflammatory mediators create tumor-promoting a microenvironment that facilitates cancer cell proliferation, angiogenesis, and metastatic progression.

The evaluation of tumor necrosis factoralpha levels revealed the complex interplay between immune system activation and cancer development, where chronic inflammation associated with kidney cancer triggers sustained TNF-α secretion by immune cells and stromal components within the tumor microenvironment. Similarly, the significant upregulation of cyclooxygenase-2 concentration reflects the activation of intracellular signaling cascades in renal cancer cells, potentially exacerbated by underlying kidney pathology such as recurrent urinary tract infections or nephrolithiasis. The elevated interleukin-6 levels further underscore the role of specific signaling pathways in renal cancer development, with genetic alterations in cancer cells and the tumor microenvironment contributing to enhanced IL-6 production and secretion. The increased LOX-2 levels this complement inflammatory profile. indicating the comprehensive activation of multiple enzymatic pathways that collectively cancer progression promote and damage.

The therapeutic efficacy of the synthesized benzofuran derivatives, particularly compound C, represents a promising advancement in targeted kidney cancer therapy. The dosedependent reductions in all inflammatory markers across treatment groups A, B, C, and D demonstrate the compounds' ability to effectively modulate the inflammatory microenvironment. Compound C emerged as the most potent inhibitor, achieving the most substantial reductions in TNF-α, COX-2, IL-6, and LOX-2 levels, which correlates directly with its superior molecular docking profile. The molecular docking studies provide crucial mechanistic insights, revealing that compound C forms four stable hydrogen bonds with target enzymes while exhibiting the most favorable binding energies across all targets, with  $\Delta G$  values of -10.6, -10.3, -8.6, and -9.8 for TNF-α, COX-2, IL-6, and LOX-2 respectively. These highly negative free energy changes indicate strong and efficient inhibitory activity, suggesting that compound C achieves optimal binding affinity and selectivity for these inflammatory enzymes.

The multitarget approach demonstrated by these benzofuran derivatives represents a significant advantage over single-target therapies, as kidney cancer involves complex, interconnected inflammatory networks that require comprehensive intervention. ability of compound C to simultaneously multiple inflammatory inhibit enzymes suggests it could effectively disrupt the positive feedback loops that sustain the tumor microenvironment, potentially leading reduced cancer cell proliferation, decreased and angiogenesis, improved treatment outcomes. Furthermore, the strong correlation between molecular docking predictions and experimental results validates the rational drug design approach employed in this study, providing confidence in the structure-activity relationships identified and supporting further optimization of these compounds. The histopathological evaluation provides compelling morphological evidence supporting the biochemical findings and further validates the therapeutic efficacy of the benzofuran derivatives in kidney cancer treatment. The control group (Group I) established the baseline normal kidney architecture, displaying intact mucosal and submucosal layers with well-defined boundaries, typical transitional epithelium morphology, and an unaffected muscular layer. In stark contrast, NDMA administration in Group II induced severe histopathological alterations characteristic of kidney cancer including luminal pathology, stenosis, extensive necrosis and desquamation of transitional epithelial cells, muscular layer thickening, and substantial inflammatory cell infiltration. These morphological changes correlate with directly the elevated inflammatory markers observed in the biochemical analysis, demonstrating the successful establishment of the kidney cancer model and the structural manifestations of chronic inflammation.

therapeutic interventions revealed varying degrees of histological recovery that aligned with the compounds' biochemical efficacy profiles. Treatment with compound A (Group III) showed moderate therapeutic benefits, with isolated epithelial degeneration and necrosis, slight mucosal and mild inflammatory thinning, infiltration, indicating partial tissue recovery compared to the severely damaged NDMAonly group. Remarkably, compound B treatment (Group IV) achieved near-complete histological restoration, with kidney tissues architecture maintaining normal resembling the control group, including intact mucosal layers lined with transitional epithelium and preserved submucosal and layers without muscular detectable histopathological damage. This exceptional therapeutic response suggests that compound B not only inhibited inflammatory pathways

but also promoted comprehensive tissue healing and regeneration.

Compound C treatment (Group V) demonstrated clear therapeutic effects with evidence of active tissue repair processes, characterized by mild mucosal thinning, limited focal inflammatory cell infiltration, and restricted cellular degeneration and necrosis. While not achieving the complete recovery observed with compound B, the histological improvements were substantial and consistent with compound C's superior biochemical profile in inflammatory marker reduction. Compound D treatment (Group VI) showed moderate therapeutic efficacy, with degeneration, vacuolar necrosis of transitional epithelial cells, and congestion, indicating partial vascular with remaining structural recovery but abnormalities.

The histopathological findings provide crucial insights into the structure-activity relationships of the benzofuran derivatives, revealing that biochemical efficacy in reducing inflammatory markers translates directly into morphological tissue recovery. The superior performance of compound B in achieving near-complete histological restoration, despite compound C showing the most potent biochemical inhibition, suggests that optimal therapeutic outcomes may require balancing multiple factors including tissue penetration, bioavailability, and cellular repair mechanisms beyond simple enzyme inhibition. These findings collectively that demonstrate benzofuran derivatives offer a promising for kidney cancer therapeutic strategy simultaneously treatment by targeting inflammatory pathways and promoting tissue recovery, with the histopathological evidence providing strong support for their clinical translation potential.

The present study demonstrates the significant therapeutic potential of novel benzofuran derivatives in targeting inflammatory pathways associated with kidney

The NDMA-induced cancer progression. kidney cancer model successfully replicated the chronic inflammatory microenvironment of renal carcinomas, characteristic evidenced by the substantial elevation of key inflammatory biomarkers including TNF-α, COX-2, IL-6, and LOX-2 compared to control groups. This inflammatory cascade represents a critical mechanism in kidney cancer sustained pathogenesis, where immune activation and the release of pro-inflammatory mediators create a tumor-promoting microenvironment that facilitates cancer cell proliferation, angiogenesis, and metastatic progression.

The evaluation of tumor necrosis factoralpha levels revealed the complex interplay between immune system activation and cancer development, where chronic inflammation associated with kidney cancer triggers sustained TNF-α secretion by immune cells and stromal components within the tumor microenvironment. Similarly, the significant upregulation of cyclooxygenase-2 concentration reflects the activation of intracellular signaling cascades in renal cancer cells, potentially exacerbated by underlying kidney pathology such as recurrent urinary tract infections or nephrolithiasis. The elevated interleukin-6 levels further underscore the role of specific signaling pathways in renal cancer development, with genetic alterations in cancer cells and the tumor microenvironment contributing to enhanced IL-6 production and secretion. The increased LOX-2 complement this inflammatory profile, indicating the comprehensive activation of multiple enzymatic pathways that collectively promote cancer progression and tissue damage.

The therapeutic efficacy of the synthesized benzofuran derivatives, particularly compound C, represents a promising advancement in targeted kidney cancer therapy. The dosedependent reductions in all inflammatory markers across treatment groups A, B, C, and D demonstrate the compounds' ability to effectively the inflammatory modulate microenvironment. Compound C emerged as the most potent inhibitor, achieving the most substantial reductions in TNF-α, COX-2, IL-6, and LOX-2 levels, which correlates directly with its superior molecular docking profile. The molecular docking studies provide crucial mechanistic insights, revealing that compound C forms four stable hydrogen bonds with target enzymes while exhibiting the most favorable binding energies across all targets, with  $\Delta G$  values of -10.6, -10.3, -8.6, and -9.8 for TNF-α, COX-2, IL-6, and LOX-2 respectively. These highly negative free energy changes indicate strong and efficient inhibitory activity, suggesting that compound C achieves optimal binding affinity and selectivity for these inflammatory enzymes.

The multitarget approach demonstrated by these benzofuran derivatives represents a advantage significant over single-target therapies, as kidney cancer involves complex, interconnected inflammatory networks that require comprehensive intervention. ability of compound C to simultaneously inhibit multiple inflammatory enzymes suggests it could effectively disrupt the positive feedback loops that sustain the tumor microenvironment, potentially leading reduced cancer cell proliferation, decreased angiogenesis, and improved treatment outcomes. Furthermore, the strong correlation between molecular docking predictions and experimental results validates the rational drug design approach employed in this study, providing confidence in the structure-activity relationships identified and supporting further optimization of these compounds. The findings collectively suggest that benzofuran derivatives, particularly compound C, offer a promising therapeutic strategy for kidney cancer treatment by targeting the inflammatory underpinnings of cancer progression, warranting continued investigation through

advanced preclinical studies and eventual clinical translation.

#### Conclusion

This study demonstrated the potential of novel benzofuran-based compounds, the particularly 6-methoxy-substituted derivative (compound C), as effective therapeutic agents against kidney cancer. Compound  $\mathbf{C}$ showed superior and anticancer inflammatory activity, levels reduced evidenced by of promarkers(COX-2,TNF-α,IL-6 inflammatory and LOX-2) and significant histological

#### References

- 1. Al-Sabawi, A. H., Younis, S. A., 2022, Synthesis of some new curcumin derivatives. In AIP Conference Proceedings (Vol. 2394, No. 1). *AIP Publishing*. doi:10.1063/5.0121197.
- 2. Tomeh, M. A., Hadianamrei, R., Zhao, X., 2019, A review of curcumin and its derivatives as anticancer agents. *International journal of molecular sciences*, 20(5), 1033. doi:10.3390/ijms20051033.
- 3. Khalaf, K. A., Omar, A. O., 2023, Green Synthesis and Spectroscopic Study of New Heterocyclic Compounds Derived from Ethyl Coumarilate. *African Journal of Advanced Pure and Applied Sciences (AJAPAS)*, 281-289.
- 4. D'arcy, M. S., 2019, Cell death: a review of the major forms of apoptosis, necrosis and autophagy. *Cell biology international*, 43(6), 582-592. doi:10.1002/cbin.11137.
- 5. Ma, J., Waxman, D. J., 2008, Combination of antiangiogenesis with chemotherapy for more effective cancer treatment. *Molecular cancer therapeutics*, 7(12), 3670-3684. doi: 10.1158/1535-7163.MCT-08-0715.
- 6. Makovec, T., 2019, Cisplatin and beyond: molecular mechanisms of action and drug resistance development in cancer chemotherapy. *Radiology and oncology*, 53(2), 148. doi: 10.2478/raon-2019-0018.

recovery. These findings suggest that benzofuran derivatives may offer a promising strategy for kidney cancer treatment through modulation of inflammation-related pathways.

#### **Conflicts of Interest**

The authors declare no conflict of interest.

### Acknowledgement

The authors are grateful for the College of Science and College of Veterinary Medicine at the University of Mosul for their provided facilities to accomplish this work.

- 7. Thoeny, H. C., Ross, B. D., 2010, Predicting and monitoring cancer treatment response with diffusion-weighted MRI. *Journal of Magnetic Resonance Imaging*, 32(1), 2-16. doi:10.1002/jmri.22167.
- 8. Zaahkouk, S. M., Aboul-Ela, E. I., Ramadan, M. A., Bakry, S., Mhany, B. M., 2015, Anticarcinogenic activity of methanolic extract of fennel seeds (Foeniculum vulgare) against breast, colon, and liver cancer cells. *Int. J. Adv. Res*, 3(5), 1525-1537.
- 9. Bray, F., Ferlay, J., Soerjomataram, I., Siegel, R. L., Torre, L. A., Jemal, A., 2018, Global cancer statistics 2018: GLOBOCAN estimates of incidence and mortality worldwide for 36 cancers in 185 countries. *CA: a cancer journal for clinicians*, 68(6), 394-424. doi:10.3322/caac.21492.
- 10. Sung, H., Ferlay, J., Siegel, R. L., Laversanne, M., Soerjomataram, I., Jemal, A., Bray, F., 2021, Global cancer statistics 2020: GLOBOCAN estimates of incidence and mortality worldwide for 36 cancers in 185 countries. *CA: a cancer journal for clinicians*, 71(3), 209-249. doi:10.3322/caac.21660.
- 11. Napiórkowska, M., Cieślak, M., Kaźmierczak-Barańska, J., Królewska-Golińska, K., Nawrot, B., 2019, Synthesis of new derivatives of benzofuran as potential anticancer agents. *Molecules*, 24(8), 1529. doi:10.3390/molecules24081529.

- 12. Abedinifar, F., Farnia, S. M. F., Mahdavi, M., Nadri, H., Moradi, A., Ghasemi, J. B., Foroumadi, A., 2018, Synthesis and cholinesterase inhibitory activity of new 2-benzofuran carboxamide-benzylpyridinum salts. *Bioorganic chemistry*, 80, 180-188. doi:10.1016/j.bioorg.2018.06.006.
- 13. Kossakowski, J., Krawiecka, M., Kuran, B., Stefańska, J., Wolska, I., 2010, Synthesis and preliminary evaluation of the antimicrobial activity of selected 3-benzofurancarboxylic acid derivatives. *Molecules*, 15(7), 4737-4749. doi:10.3390/molecules15074737.
- 14. Sehgal, S. A., 2017, Pharmacoinformatics and molecular docking studies reveal potential novel Proline Dehydrogenase (PRODH) compounds for Schizophrenia inhibition. *Medicinal Chemistry Research*, 26, 314-326. doi:10.1007/s00044-016-1752-2.
- 15. Jiang, Q., Matsuzaki, Y., Li, K., Uitto, J., 2006, Transcriptional regulation and characterization of the promoter region of the human ABCC6 gene. *Journal of investigative dermatology*, 126(2), 325-335. doi:10.1038/sj.jid.5700065.
- 16. Khalaf, A. K., Omar, O. A., 2023, Synthesis, Pharmacological Evaluation, and Docking Studies of Ethyl Coumarilate Derivatives as Potential Antibladder Cancer in a Mouse Model. *International Journal of Drug Delivery Technology*, 13(4), 1548-1556. doi:10.9734/irjpac/2022/v23i6791.
- 17. Ladokun, O. A., Abiola, A., Okikiola, D., Ayodeji, F., 2018, GC-MS and molecular docking studies of Hunteria umbellata methanolic extract as a potent anti-diabetic. *Informatics in Medicine Unlocked*, 13, 1-8. doi:10.1016/j.imu.2018.08.001. 18. Odhar, H. A., Hashim, A. F., Ahjel, S. W., Humadi, S. S., 2023, Molecular docking and dynamics simulation analysis of the human FXIIa with compounds from the Mcule database. *Bioinformation*, 19(2), 160. doi:10.6026/97320630019160.
- 19. Hassan, H. A., 2015, Synthesis of Some Benzofuran-based Pyrazoline, Isoxazoline, Pyrmidine, Cyclohexenone and Indazole Derivatives. *Iraqi National Journal of Chemistry*, 15(1), 12-26.

- 20. Gold, S. A., Margulis, V., 2023, Carcinogenic effects of nitrosodimethylamine (NDMA) contamination in ranitidine: defining the relationship with renal malignancies. *JU Open Plus*, 1(10), e00053. doi:10.1097/JU9.0000000000000058.
- 21. Hard, G. C., 1986, Experimental models for the sequential analysis of chemically-induced renal carcinogenesis. *Toxicologic pathology*, 14(1), 112-122. doi:10.1177/019262338601400114.
- 22. Erhirhie, E. O., Ekene, N. E., Ajaghaku, D. L., 2014, Guidelines on dosage calculation and stock solution preparation in experimental animals' studies. *Journal of Natural Sciences Research*, 4(18): 100-106.
- 23. Brown, A. M., 2005, A new software for carrying out one-way ANOVA post hoc tests. *Computer methods and programs in biomedicine*, 79(1), 89-95. doi:10.1016/j.cmpb.2005.02.007.
- 24. Ho, M. Y., Tang, S. J., Chuang, M. J., Cha, T. L., Li, J. Y., Sun, G. H., Sun, K. H., 2012, TNF-α induces epithelial–mesenchymal transition of renal cell carcinoma cells via a GSK3β-dependent mechanism. *Molecular cancer research*, 10(8), 1109-1119. doi:10.1158/1541-7786.MCR-12-0160. 25. Ronca, R., Van Ginderachter, J. A., Turtoi, A., 2018, Paracrine interactions of cancer-associated fibroblasts, macrophages and endothelial cells: tumor allies and foes. *Current Opinion in Oncology*, 30(1), 45-53. doi:10.1097/CCO.0000000000000000420.
- 26. Keibel, A., Singh, V., Sharma, M. C., 2009, Inflammation, microenvironment, and the immune system in cancer progression. *Current pharmaceutical design*, 15(17), 1949-1955. h doi:10.2174/138161209788453167.
- 27. He, X., Gao, Y., Hui, Z., Shen, G., Wang, S., Xie, T., Ye, X. Y., 2020, 4-Hydroxy-3-methylbenzofuran-2-carbohydrazones as novel LSD1 inhibitors. *Bioorganic & Medicinal Chemistry Letters*, 30(10), 127109. doi:10.1016/j.bmcl.2020.127109
- 28. Tabriz, H. M., Mirzaalizadeh, M., Gooran, S., Niki, F., Jabri, M., 2016, COX-2 expression in renal cell carcinoma and correlations with tumor grade, stage and patient prognosis. *Asian Pacific*

Journal of Cancer Prevention, 17(2), 535-538. doi:10.7314/APJCP.2016.17.2.535.

29. Ishibashi, K., Koguchi, T., Matsuoka, K., Onagi, A., Tanji, R., Takinami-Honda, R., Kojima, Y., 2018, Interleukin-6 induces drug resistance in renal cell carcinoma. *Fukushima journal of medical science*, 64(3), 103-110. doi:10.5387/fms.2018-15. 30. Sang, Y. B., Yang, H., Lee, W. S., Lee, S. J., Kim, S. G., Cheon, J., Kim, C., 2022, High serum levels of IL-6 predict poor responses in patients treated with pembrolizumab plus axitinib for advanced renal cell carcinoma. *Cancers*, 14(23), 5985. doi:10.3390/cancers14235985.

- 31. Chakraborty, S., Balan, M., Sabarwal, A., Choueiri, T. K., Pal, S., 2021, Metabolic reprogramming in renal cancer: events of a metabolic disease. *Biochimica et Biophysica Acta (BBA)-Reviews on Cancer*, 1876(1), 188559. doi:10.1016/j.bbcan.2021.188559.
- 32. Wang, Z., Jin, D., Zhou, S., Dong, N., Ji, Y., An, P., Luo, J., 2023, Regulatory roles of copper metabolism and cuproptosis in human cancers. *Frontiers in oncology*, 13, 1123420. doi:10.3389/fonc.2023.1123420.